Computer Methods in Biomechanics and Biomedical Engineering
Vol. 15, No. S1, September 2012, 69–71

Glottal motion and its impact on the respiratory flow

A. Scheinherr[a,b,c]*, L. Bailly[b,c], O. Boiron[a,b], T. Legou[c,d], A. Giovanni[c,d,e], G. Caillibotte[f] and M. Pichelin[f]

[a]*Centrale Marseille, IRPHE, 13451 Marseille, France;* [b]*CNRS, IRPHE, 13384 Marseille, France;* [c]*IRPHE, Aix-Marseille University, 13384 Marseille, France;* [d]*CNRS, LPL UMR6057, Aix-en-Provence, France;* [e]*Service ORL Hôpital de La Timone, CHU Marseille, Marseille, France;* [f]*Air Liquide Santé International, Groupe Gaz Médicaux, CRCD, Jouy-en-Josas, France*

Keywords: glottis; breathing; laryngofiberscopy; image processing; CFD simulations

1. Introduction

Advantages of inhaled therapies as *a priori* targeted supply of drugs make them particularly convenient for the treatment of lung diseases. Nevertheless, several physical and anatomical factors can largely influence treatment efficiency. In particular, the upper airways' anatomic arrangement acts as an unwanted filter, which limits the amount of drug delivered to the lung (Conway et al. 2012). More specifically, the glottis, defined by vocal folds aperture within the larynx, causes airways to narrow in a minimal transition cross section. This anatomical singularity yields to a complex jet-like tracheal flow (Katz et al. 1997; Renotte et al. 2000; Brouns et al. 2007), which can be determinant on particles deposition by inertial impaction. However, current studies are limited by two main issues:

- Glottal dynamics during human breathing have been barely investigated so far, and despite a few reference *in vivo* studies (Baier et al. 1977; Brancatisano et al. 1983), the relationship between glottal area and inhaled airflow is still poorly understood.
- The aerodynamic influence of the glottal geometrical changes during breathing is often discarded in numerical works. Instead, a static glottis is often considered together with steady flow conditions (Katz et al. 1997; Brouns et al. 2007).

Therefore, the aim of this study was (i) to characterise the glottal dynamics during human breathing *in vivo* using laryngofiberscopy and synchronised airflow recordings and (ii) to quantify the effects of a mobile glottis and unsteady flow conditions on laryngeal jet-flow dynamics using CFD modelling.

2. Methods

2.1 In vivo *study*

In vivo experiments were conducted in the ENT Department of La Timone Hospital. One healthy female volunteer (LB, age 29 years) and one healthy male volunteer (OB, age 48 years) were recorded while performing two 30-s breathing tasks: normal breathing (*eupnea*) and forced breathing (*tachypnea*). Laryngofiberscopic investigations were made using a flexible nasofiberscope (Storz 202220 20 tricam camera) with a continuous cold light source and a colour CCD camera. Laryngeal images were captured with a camera frame rate of 25 frames/s and an image resolution of 768×288 pixels. The oral airflow signal was simultaneously registered by means of a pneumotachograph placed at the mouth, EVA2 (Ghio and Teston 2004).

2.2 In silico *study*

As a first approximation of the glottal geometry was built a 2D rectangular moving constriction with a triangular dynamic mesh of 24,000 el. The mesh density ensures grid-independent results. CFD simulations were conducted using Fluent 6.3.26 under laminar airflow conditions, assuming an incompressible Newtonian gas of viscosity ν equal to 1.789×10^{-5} kg/ms. A pressure outlet boundary condition was set to 0 Pa. Unsteady boundary conditions comprising the glottal width $d_g(t)$ and the velocity inlet were parametrically varied in agreement with the *in vivo* study. A no-slip shear boundary condition was applied at solid walls. Initially, zero velocities and pressures were assumed at all points. Equations were solved using a first-order time and spatial discretisation schemes, and a time step set to 0.12 s.

3. Results and discussion

3.1 *Airflow rate*

In vivo measurements yielded to about 30 respiratory cycles during *eupnea* and 40 during *tachypnea*. Every respiratory cycle was detected using a zero-tracking method developed in Matlab R2011b. Each airflow signal

*Corresponding author. Email: scheinherr@irphe.univ-mrs.fr

ISSN 1025-5842 print/ISSN 1476-8259 online

http://dx.doi.org/10.1080/10255842.2012.713685
http://www.tandfonline.com

Q was normalised with respect to the maximum value achieved within the cycle, Q_{max}. Time t was normalised by corresponding respiratory period, $T = 2\pi/\omega$. The maximal period registered within each 30-s sequence is denoted as T_{max}. Signals were finally averaged into one mean flow-rate, herein denoted as $<Q/Q_{max}>$. Figure 1(a) illustrates the typical flow-rate $<Q/Q_{max}>$ as a function of ωt, produced by subject OB during *eupnea* (maximal $Q_{max} = 1.9\,\mathrm{dm^3/s}$, $T_{max} = 0.62\,\mathrm{s}$) and *tachypnea* (maximal $Q_{max} = 4.3\,\mathrm{dm^3/s}$, $T_{max} = 4.8\,\mathrm{s}$). In comparison, a sinusoidal evolution is plotted. Conventionally, positive (respectively, negative) flow-rate values correspond to expiration (respectively, inspiration) phase. During *eupnea*, the inspiration and expiration curves are similar (up to sign) and their durations are approximately equal, as commonly found in the literature (Fenn and Rahn 1965). During *tachypnea*, the mean flow-rate curve deviates from the harmonic signal although inspiration and expiration durations remain roughly equal. A phase difference of about 22° in flow-rate maximal occurrences has been measured between sinusoid and *eupnea* curve, which corresponds to 6% of the breathing period. The phase difference increases during *tachypnea* up to 58°, namely 16% of the cycle duration. LB breathing shows similar characteristics.

3.2 Glottal motion

Glottal motion was extracted from the laryngoscopic images using Matlab Image Processing Toolbox and different phases: (i) focus on a region of interest using a cross-correlation technique, (ii) smoothing using a specific filter function (Kroon 2009), (iii) detection of the glottal contours using a segmentation method (Bernard et al. 2009), (iv) measurement of the glottal antero-posterior diameter AP_g, glottal area A_g and glottal width d_g (see Figure 1(b)), (v) normalisation by comparing AP_g diameter with the initial value AP_g^0, assumed as a geometrical invariant (Higenbottam 1980), and (vi) conversion from pixels to millimeters, assuming $AP_g = 22\,\mathrm{mm}$ (Conway et al. 2012).

Figure 1(c) illustrates the evolution of the glottal dynamics measured during a typical *eupnea* cycle. Glottal area A_g and glottal width d_g are displayed as function of time, together with synchronised airflow rate Q. It is shown that the glottis progressively widens during inspiration and

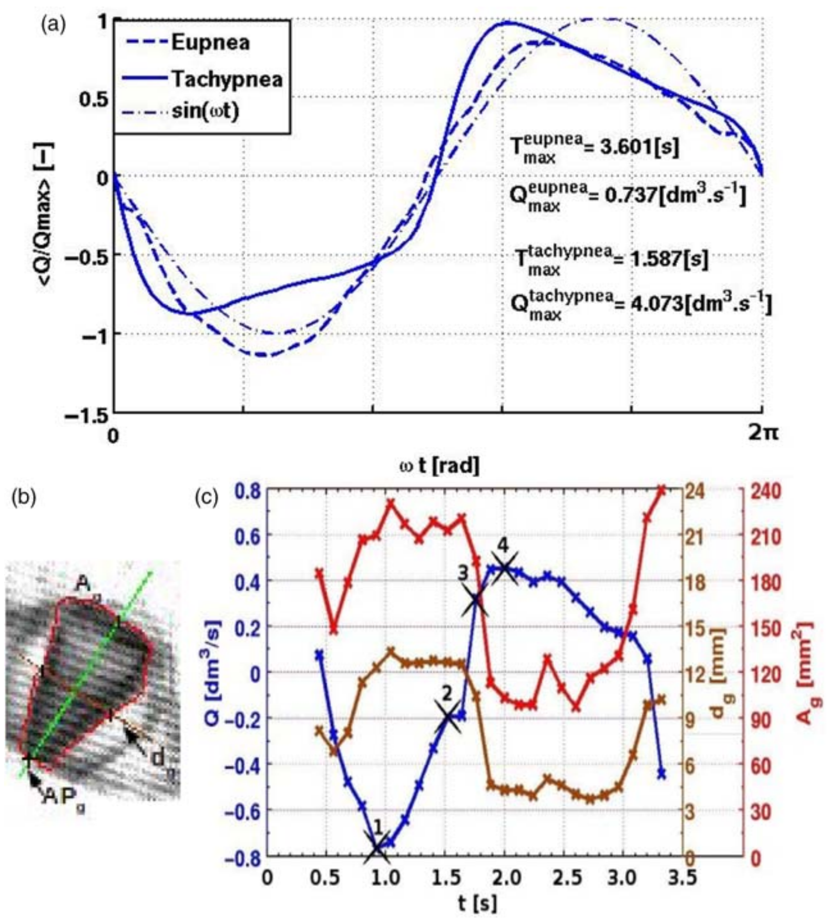

Figure 1. (a) Mean flow-rate $<Q/Q_{max}>$ measured during cycles of eupnea and tachypnea (subject OB) and comparison with sinusoid. (b) Illustration of glottal image post-processing. (c) Detected glottal area A_g, glottic width d_g and flow-rate Q.

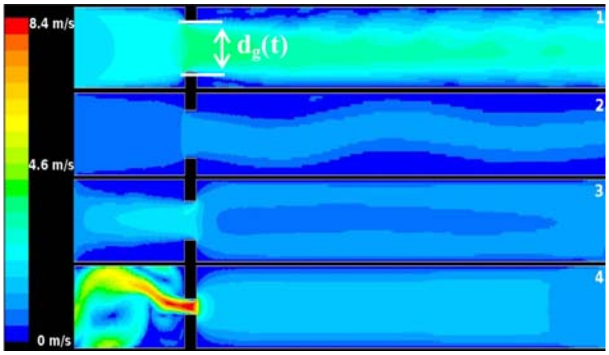

Figure 2. 2D unsteady simulations of velocity field through the moving glottis during a breathing cycle.

narrows during expiration. Area A_g varies in the range 90–240 mm^2 (mean value 165 mm^2) during the cycle, while d_g varies in the range 4–13 mm (mean value 7.8 mm), thus achieving a peak value during inspiration nearly three times greater than that measured during expiration. This ratio is in line with previous studies (Baier et al. 1977; Brancatisano et al. 1983). The above measurements allowed the assessment of a Reynolds number ($\mathrm{Re} = \{d_g Q\}/\{\nu A_g\}$) ranging from 500 to 2500.

3.3 CFD simulations

Unsteady flow simulations were carried out considering Q and d_g measured during the typical *eupnea* cycle (Figure 1(c)). Figure 2 shows the development of the glottal jet at four shot-instants at first during inspiration and consequently during expiration phase of breathing (crosses in Figure 1(c)). Inertial effects associated with flow-rate variations yield to the jet instability and fluctuations of the reattachment area during the breathing cycle but the flow despite $\mathrm{Re} \cong 2500$ stays laminar as already noticed in Boiron et al. (2007).

4. Conclusions

The *in vivo* study showed that the glottis can be extremely variable during breathing and hence influence airflow characteristics. A glottal area widening was quantified during inspiration, with a typical ratio of 3:1 as compared to expiration. Airflow rate variations differ from harmonic signal during *eupnea* as well as *tachypnea*. The correlation between flow-rate and glottal area will be discussed and compared to previous clinical investigations. Preliminary 2D CFD simulations of the glottal jet were carried out based on the measured flow-rate and glottal changes during *eupnea*. Impact of unsteady flow conditions on the jet development is demonstrated.

References

Baier H, Wanner A, Zarzecki S, Sackner MA. 1977. Relationships among glottis opening, respiratory flow and upper airway resistance in humans. J Appl Physiol. 43: 603–611.

Bernard O, Friboulet D, Thévenaz P, Unser M. 2009. Variational B-spline level-set: a linear filtering approach for fast deformable model evolution. IEEE Trans Image Process. 18:1179–1191.

Boiron O, Deplano V, Pelissier R. 2007. Experimental and numerical studies on the starting effect on the secondary flow in a bend. J Fluid Mech. 574:109–129.

Brancatisano T, Collett P, Engel L. 1983. Respiratory movements of the vocal cords. J Appl Physiol. 54(5):1269–1276.

Brouns M, Verbanck S, Lacor C. 2007. Influence of glottal aperture on the tracheal flow. J Biomech. 40:165–172.

Conway J, Fleming J, Majoral C, Katz I, Perchet D, Peebles C, Tossici-Bolt L. 2012. Controlled, parametric, individualized, 2-d and 3-d imaging measurements of aerosol deposition in the respiratory tract of healthy human subjects for model validation. J Aerosol Sci. 52:1–17. DOI: 10.1016/j.jaerosci.2012.04.006.

Fenn WO, Rahn H. 1965. Handbook of physiology, section 3: respiration. Washington, DC: American Physiological Society.

Ghio A, Teston B. 2004. Evaluation of the acoustic and aerodynamic constraints of a pneumotachograph for speech and voice studies. In: Proceedings of International Conference on Voice Physiology and Biomechanics. Marseille, France: Univeristy of Méditerranée. p. 55–58.

Higenbottam T. 1980. Narrowing of glottis opening in humans associated with experimentally induced broncho-constriction. J Appl Physiol. 49:403–407.

Katz I, Martonen T, Flaa W. 1997. Three-dimensional computational study of inspiratory aerosol flow through the larynx: the effect of glottal aperture modulation. J Aerosol Sci. 28:1073–1083.

Kroon DJ. 2009. Hessian based frangi vesselness filter – matlab code. University of Twente, Hollande.

Renotte C, Bouffioux V, Wilquem F. 2000. Numerical analysis of oscillatory flow in the time-varying laryngeal channel. J Biomech. 33:1637–1644.